Heat Mass Transfer (2010) 46:695–706
DOI 10.1007/s00231-010-0620-8

ORIGINAL

Effect of inclination angle on the pool boiling heat transfer of ultra-light copper foams

Yongping Yang · Xianbing Ji · Jinliang Xu

Received: 8 October 2009 / Accepted: 23 May 2010 / Published online: 5 June 2010

Abstract Effect of inclination angles on the pool boiling heat transfer on ultra-light copper foam covers was studied using acetone as the working fluid. The inclination angle was from 0° to 90°. It is found that copper foam covers decrease the surface superheat at the onset of nucleate boiling and extend the operation ranges of surface superheats and heat fluxes, significantly. Boiling curves are crossed between low and high inclination angles. Heat transfer coefficients are increased, attain maximum values, and then are decreased with continuous increases in heat fluxes. The thermal performance is very insensitive to inclination angles at low pool liquid temperatures. The thermal performance is better for the saturation pool boiling heat transfer at small surface superheats, but it is better for the subcooled pool boiling heat transfer at high surface superheats. The Nusselt number is well correlated using the 812 data points, with the maximum error of 20%.

List of symbols

a_0, a_1 and a_2	Empirically determined constants for temperature distribution in copper block
ANG	The parameter describing the effect of inclination angles
Bo	Bond number
C_{pf}	Specific heat of liquid J kg^{-1} K^{-1}
d_{f}	Copper ligament diameter mm
d_{p}	Pore diameter of copper foam mm
F	The F number, defined as δ/d_{p}
g	Gravity force acceleration m s^{-2}
h	Heat transfer coefficient W m^{-2} K^{-1}
h_{fg}	Latent heat of evaporation J kg^{-1}
$k_{\mathbf{e}}$	Effective thermal conductivity for copper foam solid–liquid system W m^{-1} K^{-1}
$k_{\mathbf{f}}$	Thermal conductivity of liquid W m^{-1} K^{-1}
$k_{\mathbf{s}}$	Thermal conductivity of solid copper W m^{-1} K^{-1}
l	Ligament length of a unit cell m
$m_{\mathbf{g}}$	Mass flux of vapor phase kg m^{-2} s^{-1}
Nu	The Nusselt number
ppi	The number of pores per unit length of foam cell
q	Heat flux at the base surface W m^{-2}
Re	The vapor Reynolds number
Ste	The Stefan number
T	Temperature K or °C
u_{v}	Vapor velocity m s^{-1}
V	Volume of a foam cell m^3
z	Coordinate perpendicular to the base surface m
$\frac{dT}{dz}\|_{\text{base surface}}$	Temperature gradient at the base surface K m^{-1}
δ	Thickness of foam cover m
ΔT_{sat}	Wall superheat K or °C
ε	Porosity of foam cover
θ	Inclination angles of heating surface with respective to the horizontal position o
μ	Dynamic viscosity Pa s
v	Kinematic viscosity m^2/s
ρ	Density kg m^{-3}
σ	Surface tension force N m^{-1}
Θ	Pool liquid subcooling effect

Y. Yang · X. Ji · J. Xu (✉)
Beijing Key Laboratory of New and Renewable Energy,
North China Electric Power University,
Beijing 102206, People's Republic of China
e-mail: xjl@ncepu.edu.cn

Subscripts

Bulk	Pool bulk condition
f	Liquid phase
g	Vapor phase
sat	Saturation condition
w	Wall surface condition

1 Introduction

Pool boiling heat transfer with porous surface has been widely used in power, chemical, and electronic engineering to dissipate high heat flux. High integration of microelectronic components yields the increased heat flux on the chip surface that is to be dissipated, under which compact heat transfer devices are expected. Ultra-light metallic foam is a kind of porous media having low density, high porosity, and large surface to volume ratio, offering multifunctions of sound-absorbing, noise reduction and electromagnetic shielding. Besides, metallic foam is a good material that can be used in heat transfer devices [1, 2]. Effective thermal conductivity [3, 4], thermal radiation heat transfer [5], single-phase flow and heat transfer [6, 7] have been studied for the metallic foams. However, few studies of pool boiling heat transfer on metallic foam covers can be found in the literature [8–10].

The review papers by Thome [11], Bergles [12], and Ingham and Pop [13] show that surface temperatures of the pool boiling heat transfer can be decreased by porous coatings. The heat flux is increased at the same surface superheat by increasing the active nucleation sites and/or the bubble detaching frequencies [14, 15]. Metallic foams with high porosity and good connectivity of pores show distinct boiling heat transfer performance to other structures such as porous powder. Arbelaez et al. [16] performed pool boiling experiments on aluminum foam covers with pore densities in the range of 5–40 ppi. Heat transfer enhancement is observed for the low porosity when the value of ppi is fixed. The transition from nucleate boiling to stable film boiling is marked by a small temperature overshoot. Boiling hysteresis is absent at the Onset of Nucleate Boiling (ONB). Moghaddam and Ohadi [17] studied pool boiling heat transfer of water and FC-72 on metallic and graphite foam covers attached on a high heat flux surface. It was shown that significant heat transfer enhancement is achieved for the boiling of water on the 30 ppi copper foam cover, but no enhancement was observed on the 80 ppi copper and the graphite foam covers. However, a substantial heat transfer enhancement was observed on all foam covers for the boiling of FC-72. Xu et al. [9] performed high speed visualization and pool boiling heat transfer studies on copper foam covers using acetone as the working fluid over wide parameter ranges. Boiling curves of copper foams show three distinct regions, and are inter-crossed between low and high ppi foams. Cage bubbles were observed.

Effect of inclination angles of the heating surface on the pool boiling heat transfer was studied on plain surfaces in [18–20]. It is shown that the heat transfer performance is influenced by inclination angles significantly. Chang and You [21] and Rainey and You [22] show that unlike the plain surfaces, the nuclear boiling curves of the microporous enhanced surfaces were insensitive to both inclination angle and heater sizes provided by the surface microstructure. El-Genk and Parker [23] investigated saturated and subcooled pool boiling heat transfer on graphite foam covers at inclination angles of 0°(upward facing) to 180° (downward facing), using FC-72 and HFE-7100 as the working fluids. The results show that the inclination angles have great effect on the pool boiling heat transfer. The pool boiling heat transfer is enhanced with increases in inclination angles at surface superheats smaller than 15 K. But it is deteriorated with increases in inclination angles at higher surface superheats. Athreya et al. [10] noted that boiling heat transfer on metallic foam covers is different at horizontal and vertical orientations. But their experiment did not involve other inclination angles.

The objective of this paper is to study the effect of inclination angles on the pool boiling heat transfer. Experiments were performed on the copper foam covers using acetone as the working fluid with the surface area of 12.0 mm by 12.0 mm. The pore densities are 30, 60, and 90 ppi and porosity is 0.88. Three foam cover thicknesses of 3.0, 4.0 and 5.0 mm are tested. The inclination angles are varied from 0° to 90°. It is found that copper foam covers not only decrease the surface superheat at the onset of nucleate boiling (ONB), but also extend the operation ranges of surface superheats and heat fluxes, significantly. Boiling curves are crossed between low and high inclination angles. With increases in inclination angles the thermal performance becomes poorer at small or moderate surface superheats or heat fluxes, but becomes better at larger surface superheats or heat fluxes. Heat transfer coefficients are increased, attain maximum values, and then are decreased with continuous increases in heat fluxes. The thermal performance is very insensitive to inclination angles at the low pool liquid temperatures. The Nusselt number is well correlated using the 812 data points, with the maximum error of 20%.

2 Experiments

2.1 The experimental setup

Figure 1 shows the experimental setup. A rectangular chamber (5) was made by bonding four glass side walls with

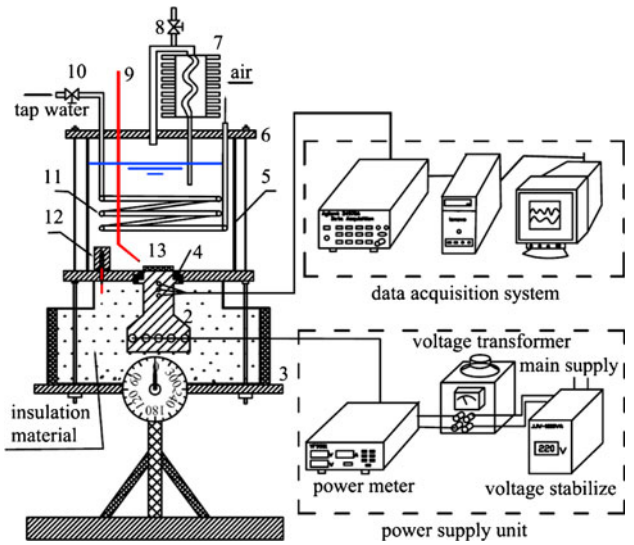

Fig. 1 The experimental setup (*1* insulation material; *2* copper block; *3* bottom stainless steel plate; *4* Teflon and epoxy glue; *5* rectangular chamber; *6* top stainless steel plate; *7* condenser; *8* pressure release valve; *9* K-type thermocouple; *10* regulating valve; *11* coiled copper tube; *12* auxiliary heater; *13* copper foam)

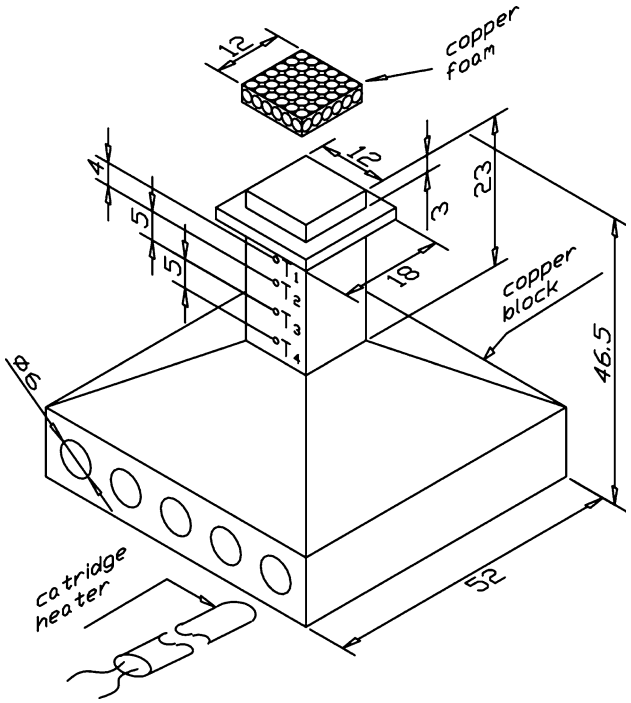

Fig. 2 The test section (all dimensions in mm)

top and bottom stainless steel plates (6). The chamber had the size of 125.0 × 127.0 × 145.0 mm^3. The thickness is 2.0 mm for the top stainless steel plate but it is 3.0 mm for the bottom one. There is a rectangular hole drilled in the center of the bottom stainless steel plate. The copper block (2) was adapted with the bottom stainless steel plate by filling the Teflon and epoxy glue (4) between them, ensuring the copper foam (13) immersed in the pool liquid and good thermal insulation, and preventing the liquid leakage. The copper block is surrounded by the insulation material of glass sheath to reduce the heat loss to the environment. There are a coiled copper tube (11) and an auxiliary heater (12) in the rectangular chamber, by which the pool liquid temperature can be adjusted and fixed at a desired value. There is a condenser (7) located at the top of the glass chamber. The vapor in the condenser is condensed by forced convective air through a fin heat sink at the outside of the condenser. The condensed liquid returns to the glass chamber by gravity.

A power supply unit is used to heat the test section, consisting of a 220 V power supplier, a voltage transformer and a power meter. The whole experimental setup was positioned on an inclination angle adjustment rig. The inclination angles can be changed from 0 to 90°. The zero degree of the inclination angle refers to the horizontally positioned heating surface, while the 90° inclination angle refers to the vertically positioned heating surface.

2.2 The test section

The test section was made of copper and its geometry and dimensions are shown in Fig. 2. It is 46.5 mm in height. Its top surface has a rectangular shape with the size of 12.0 × 12.0 mm^2. In the middle part of the copper block there are four 1.0 mm diameter holes in which four K-type thermocouples are inserted. The distance between two adjacent holes is 4.0, 5.0 and 5.0 mm, respectively from top to bottom. In the bottom part of the copper block there are five 6.0 mm diameter holes, in which five cartridge heaters are inserted, providing a maximum power of 500 W totally for the test section.

Because the copper foam cover is welded on the copper surface, the contact resistance between the copper foam and the copper surface is neglectable. Before the welding process, the copper block and copper foam cover were cleaned and baked in an oven, and then taken out of the oven. The copper block was heated by the five cartridge heaters until its temperature reached the melting temperature of the tin, leaving a thin tin thickness on the copper surface. The copper foam cover was put on the copper surface, and was tightly welded with the copper surface by turning off the heating power.

2.3 The copper foam

Figure 3a–c shows the three copper foam samples used in our experiment, having the porosity of 0.88 and the ppi of 30, 60 and 90. The copper foam has open-celled structure composed of dodecahedron-like cells, having 12–14 pentagonal or hexagonal faces. The ligament cross section

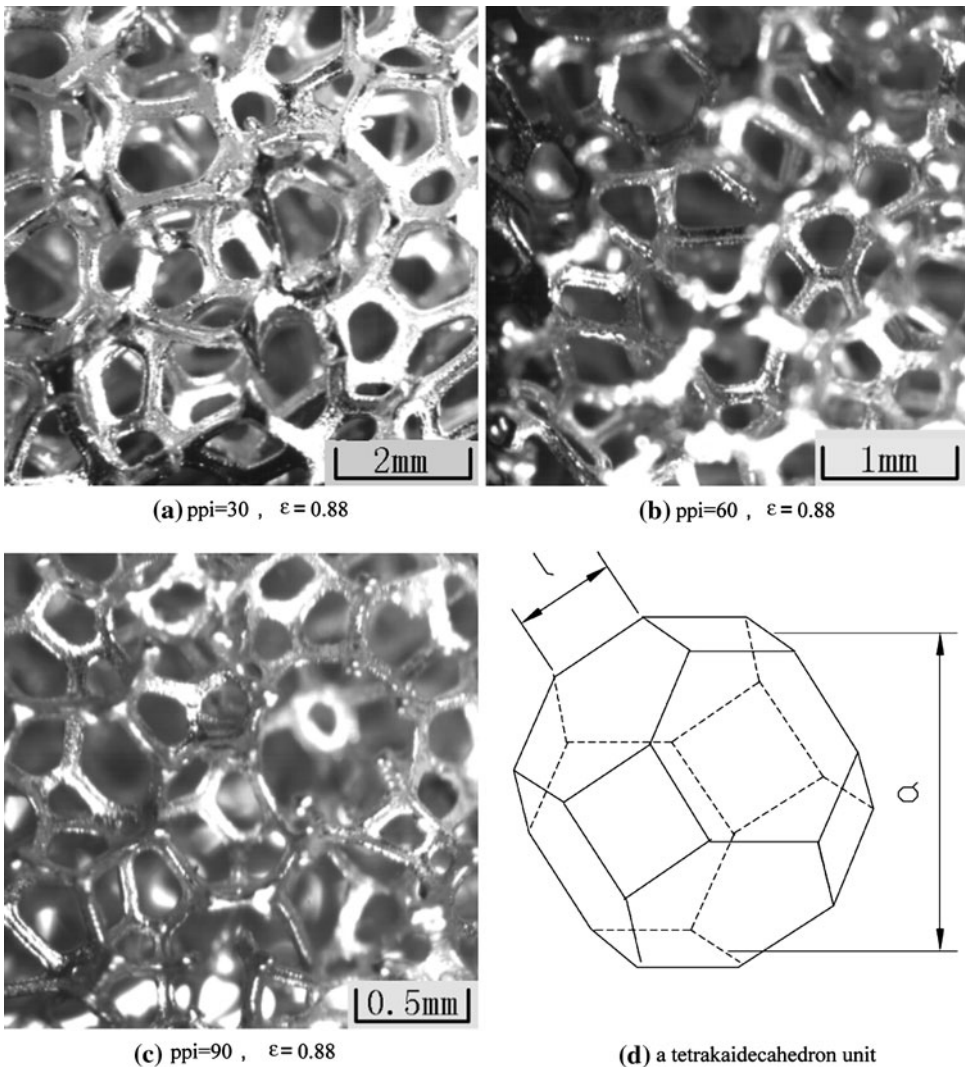

Fig. 3 The photos of copper foams (**a**, **b**, and **c**) and a unit foam cell represented by a tetrakaidecahedron unit (**d**)

(**a**) ppi=30 , ε = 0.88

(**b**) ppi=60 , ε = 0.88

(**c**) ppi=90 , ε = 0.88

(**d**) a tetrakaidecahedron unit

depends on porosity (ε), and changes from a circle at $\varepsilon = 0.85$ to an inner concave at $\varepsilon = 0.97$ [24]. A unit cell of the foam is shown in Fig. 3d, with the assumed tetrakaidecahedron shape. The ligament length is l with its diameter of d_f. Thus the volume of a unit cell is $V = 8\sqrt{2}l^3$. The circumcircle diameter of the foam cell is $\sqrt{10}l$ [14], which can be regarded as the pore diameter of d_p, i.e., $d_p = \sqrt{10}l$, not considering the ligament thickness.

The foam cell parameters were measured by a Leica M-type microscope (Germany) and are given in Table 1. The larger the ppi, the smaller the pore diameter of d_p and ligament diameter of d_f are. At the given porosity of 0.88, although the ppi is different, the value of d_f/d_p close to a constant for the metal foam covers used in this experiment. We examined the validity of the correlation of $d_p = \sqrt{10}l$. It is seen that the measured ligament length l deviates from the calculated value of $l = d_p/\sqrt{10}$ by 20% if we do not consider the ligament thickness, from Table 1. The difference between the measured and computed values regarding l becomes 10% if we consider the ligament thickness.

2.4 The experimental procedure

It is known that pool boiling heat transfer is influenced by the non-condensable gas in the liquid. Before formal experiment, the pool liquid was boiled by the auxiliary heater for 1 h to remove the non-condensable gas. Acetone has a lower saturation temperature of $T_{sat} = 56.3$°C at atmospheric pressure compared with other liquids such as water. Other physical properties of acetone are shown in Table 2.

During each experiment, the pool liquid temperature and the inclination angle were fixed at desired values. The heat flux (defined at the top base copper surface) was increased by 1–2 W/cm^2 for each step. If the recorded temperatures of the copper block had fluctuations of <0.5°C in 1 min, a steady heat transfer state is thought to be reached. In order

Table 1 The major foam structure parameters that were used in the present paper

ppi	ε	d_p (mm)	l (mm)	d_f (mm)	d_f/d_p
30	0.88	2.762	1.074	0.314	0.114
60	0.88	1.192	0.486	0.141	0.118
90	0.88	0.696	0.275	0.081	0.116

to capture the heat transfer state at the Onset of Nucleate Boiling (ONB), a much smaller heat flux increment such as 0–1 W/cm^2 was used around the boiling incipience.

2.5 Data deduction and uncertainty analysis

The one-dimensional thermal conduction equation was used to compute the heat flux as $q = -k\frac{dT}{dz}\big|_{\text{base surface}}$, where k is the copper thermal conductivity, $\frac{dT}{dz}\big|_{\text{base surface}}$ is the temperature gradient at the base surface, z is the coordinate perpendicular to the base surface. The heat flux uncertainty was estimated to be smaller than 6.0%. A least square correlation of temperatures versus z was written as $T = a_0 + a_1 z + a_2 z^2$, where a_0, a_1, and a_2 are constants correlated based on T_1, T_2, T_3 and T_4 (see Fig. 2). The surface superheat ΔT_{sat} is defined as the surface temperature of T_w subtracting T_{sat}, where T_w is the temperature at the base surface, T_{sat} is the saturation temperature of acetone at atmospheric pressure. Heat transfer coefficient is computed as

$$h = q/(T_w - T_{\text{bulk}}) \tag{1}$$

where T_{bulk} is the pool liquid temperature. The surface temperature, surface superheat, and pool liquid temperature have the maximum uncertainties of 0.3°C.

We estimate the uncertainty of heat transfer coefficient, which is a function of three independent variables of q, T_w, and T_{bulk}. The uncertainty of h is computed as

$$\Delta h = \sqrt{\left(\frac{\partial h}{\partial q}\right)^2 \Delta q^2 + \left(\frac{\partial h}{\partial T_w}\right)^2 \Delta T_w^2 + \left(\frac{\partial h}{\partial T_{\text{bulk}}}\right)^2 \Delta T_{\text{bulk}}^2} \tag{2}$$

Thus the relative uncertainty can be calculated by substituting Eq. 1 into Eq. 2 as

$$\frac{\Delta h}{h} = \sqrt{\left(\frac{\Delta q}{q}\right)^2 + \left(\frac{\Delta T_w}{T_w - T_{\text{bulk}}}\right)^2 + \left(\frac{\Delta T_{\text{bulk}}}{T_w - T_{\text{bulk}}}\right)^2} \tag{3}$$

In Eqs. 2–3, Δq, ΔT_w, and ΔT_{bulk} are the uncertainties of heat flux, wall surface temperature and pool liquid temperature. The maximum uncertainty of h is reached by a smaller surface temperature and a larger pool liquid temperature. Thus the maximum relative uncertainty of h is estimated to be 8.52%.

This study covers the following data ranges: ppi of 30, 60, 90; porosity of 0.88; foam cover thickness of 3.0, 4.0 and 5.0 mm; surface superheat from −20 to 160 K; surface heat flux up to 140 W/cm^2. The inclination angles are varied from 0° (horizontally positioned heating surface) to 90° (vertically positioned heating surface). It is noted that the heat flux is based on the top copper surface area of 12.0 mm by 12.0 mm. The foam cell area is not involved in the computation of heat flux.

3 Results and discussion

3.1 Effect of inclination angle

Figure 4 shows the effect of inclination angles on the boiling curves for the pore density of 30, 60 and 90 ppi, foam cover thicknesses of 3.0 mm and pool liquid temperature of 55°C, approaching the saturation temperature of acetone at atmospheric pressure. Later we will show the boiling curves at low pool liquid temperatures. It is found from Fig. 4 that the copper foam covers significantly decrease the surface superheats at the Onset of Nucleate Boiling (ONB). For comparison, the plain surface needs the surface superheat of about 21 K for the ONB. In contrast, the surface superheats are about 10 K for the ONB when copper foam covers are used. The boiling hysteresis phenomenon is observed when the heating surface is nearly vertically positioned ($\theta = 60$ and 90°) for the 60 ppi foam covers (see Fig. 4b), but it is not observed for the 90 ppi foam covers (see Fig. 4c).

It is shown from Fig. 4 that the critical heat flux (CHF) is approached when the surface superheat attains 38 K for the plain surface. The CHF is not reached until very high surface superheats of about 100 K for 30 and 60 ppi foam covers and 160 K for 90 ppi foam covers. The copper foam covers significantly extend the operation range of surface superheats.

It is noted that the boiling curves are crossed between the low and high surface inclination angles, i.e., the thermal performance becomes poorer with increases in surface inclination angles at low surface superheats, but it becomes better with increases in surface inclination angles at higher

Table 2 The physical properties of acetone at the atmosphere pressure

T_{sat} (°C)	ρ_f (kg/m^3)	C_{pf} (J/kgK)	C_{pg} (J/kgK)	h_{fg} (kJ/kg)	σ (N/m)	μ_f (Pa s)	k_f (W/mK)
56.29	748.01	2,302.5	1,380.6	512.94	0.0192	0.000237	0.518

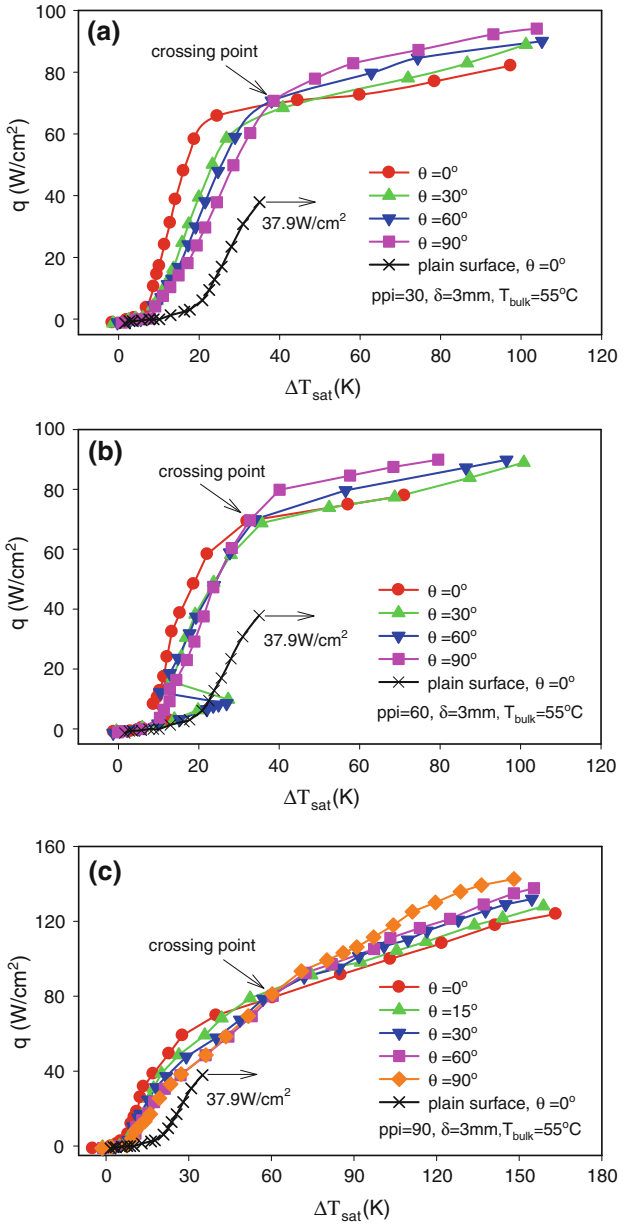

Fig. 4 Effect of inclination angle on *boiling curves* at the pool liquid temperature of 55°C

surface superheats. In each subfigures to Fig. 4, almost all the boiling curves are crossed at the same point. For instance, the boiling curves are crossed at the point of $\Delta T_{sat} = 32$ K and $q = 69$ W/cm^2 for the 60 ppi foam covers, while they are crossed at the point of $\Delta T_{sat} = 60$ K and $q = 79$ W/cm^2 for the 90 ppi foam covers. The cross point strongly depends on the pore density of ppi.

Pool boiling heat transfer is governed by the bubble nucleation sites, vapor (or bubble) release resistance, and liquid suction. The boiling heat transfer is mainly controlled by the bubble nucleation sites and bubble release resistance at low heat flux or surface superheat, but it is controlled by the liquid suction towards the heating surface at high heat flux or surface superheat. The crossing of boiling curves between low and high inclination angles is explained as follows. When the heat flux or surface superheat is low, the generated bubbles are more freely to escape to the pool liquid for the horizontally positioned heating surface than those for the vertically positioned one. In other words, the vertically positioned heating surface creates a larger bubble detachment resistance thus the heat transfer performance is poorer. This situation is changed when a high heat flux or surface superheat is applied on the heating surface, under which liquid suction toward the heating surface (foam cells) is important to maintain the heating surface covered by the liquid film. A vertically positioned heating surface is helpful to create a significant buoyancy force to suck the liquid from the bottom of the heating surface, thus it has better thermal performance than that with horizontally positioned heating surface.

In order to further identify the effect of inclination angles on the pool boiling heat transfer with or without foam covers, heat transfer coefficients are plotted versus heat flux for the plain surface, 30, 60 and 90 ppi foam covers in the four subfigures of Fig. 5. Generally these curves illustrate parabolic shape, i.e., heat transfer coefficients are increased, attain maximum values, and then are decreased with continuous increases in heat fluxes. This trend is similar to our previous studies for pool boiling heat transfer of copper foam covers with horizontally positioned heating surface [9]. Consistent with the boiling curves shown in Fig. 4, heat transfer coefficients are slightly higher for the lower inclination angles than those for the higher inclination angles when heat fluxes are small or moderate, but they are higher for the higher inclination angles at large heat fluxes.

3.2 Effect of foam cover thickness

The increased foam cover thickness increases the extended surface area of foam cells, influencing the pool boiling heat transfer. Figure 6 gave the boiling curves for the foam cover thickness of 3.0, 4.0 and 5.0 mm. Generally boiling curves show small differences for the three foam cover thicknesses. The foam cover thickness of 5.0 mm yields the better thermal performance for the surface superheats <20–25 K, i.e., ΔT_{sat} <20–25 K, due to the more extended heat transfer area and bubble nucleation sites. However, the thermal performance is better for the foam cover thickness of 3.0 mm if the surface superheats are larger than 20–25 K. When the applied heat fluxes or surface superheats are high, the larger foam cover thickness increases the vapor release resistance, deteriorating the heat transfer performance. Boiling hysteresis is only observed for the

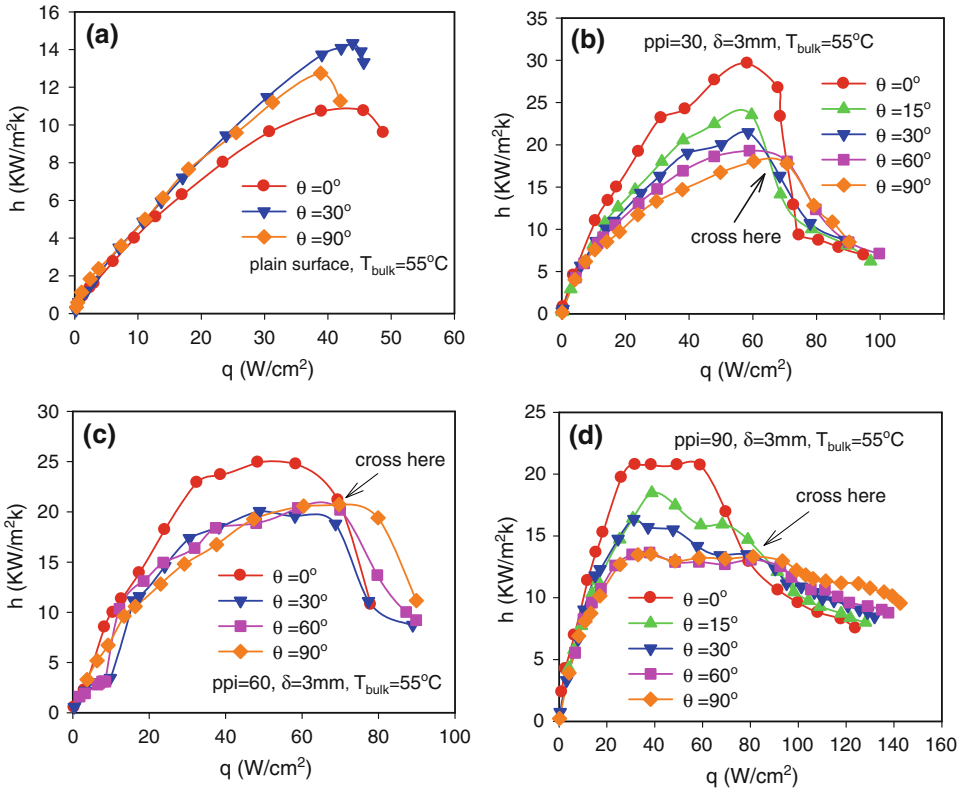

Fig. 5 Effect of inclination angle on heat transfer coefficients of plain surface and copper foam covers

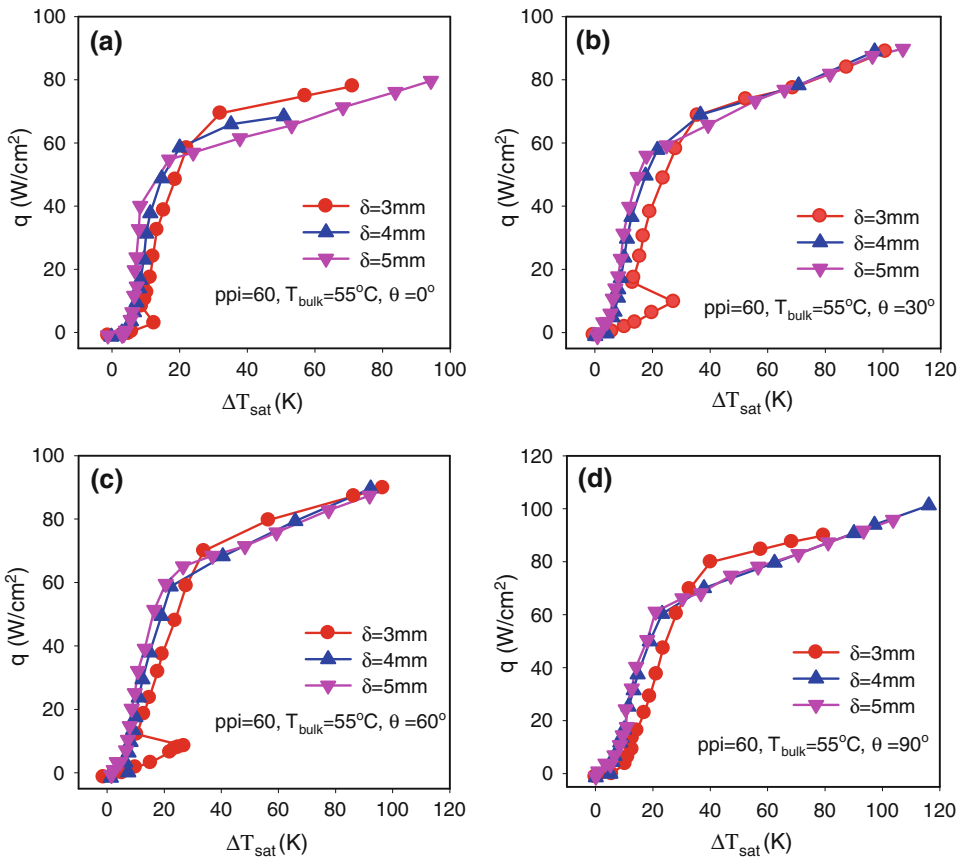

Fig. 6 Effect of copper foam cover thickness on *boiling curves* at various inclination angles

foam cover thickness of 3.0 mm, but not found for the foam cover thicknesses of 4.0 and 5.0 mm.

3.3 Effect of pool liquid temperature

Figures 4, 5, 6 demonstrate the pool boiling heat transfer at the pool liquid temperature of 55°C. The pool liquid temperature of 55°C approaches the saturation temperature of acetone at atmospheric pressure. Now we explore the effect of pool liquid temperatures on the pool boiling heat transfer on foam covers. It is shown in Fig. 7 that the pool boiling heat transfer is very insensitive to inclination angles at the low pool liquid temperature of 38°C. Under the low pool liquid temperatures, the generated bubbles are easily condensed in foam cells, causing the heat transfer insensitive to the inclination angles.

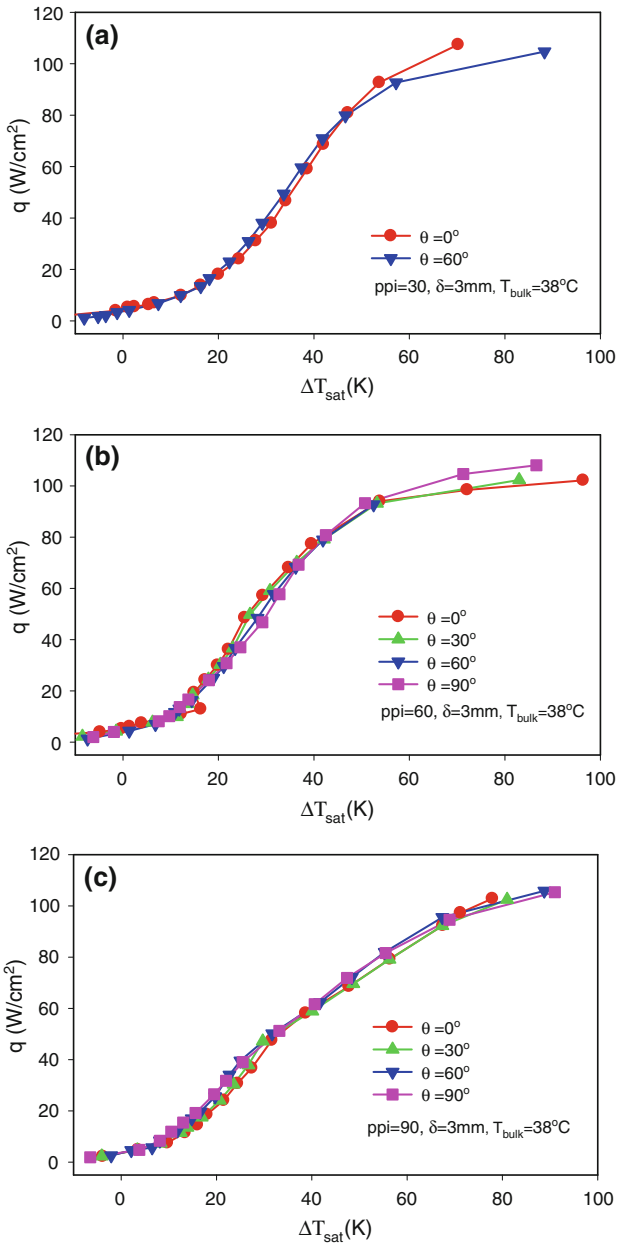

Fig. 7 Effect of inclination angle on *boiling curves* at low pool liquid temperature of 38°C

Figure 8 shows the boiling curves for ppi = 60, δ = 3.0 mm with the four inclination angles of 0°, 30°, 60° and 90°. Three pool liquid temperatures of 38, 48 and 55°C are presented. Figure 8 shows that the heat transfer performance is slightly better at the higher pool liquid temperature of 55°C for small or moderate surface superheats, but it is better at the lower pool liquid temperature of 38°C for high surface superheats. At low surface superheats, the higher pool liquid temperature cause the easy bubble generation in foam cells, leading to the enhanced heat transfer. However, at high surface superheats, the lower pool liquid temperature causes the condensation effect on the generated bubbles in foam cells, decreasing the vapor release resistance to yield better thermal performance.

3.4 Boiling hysteresis

In this study, boiling curves were obtained by the heat-flux-increase route. The phenomenon of boiling hysteresis refers to a temperature excursion at the onset of nucleate boiling (ONB) when heat flux is gradually increased. A sharp temperature decrease takes place just beyond the ONB, followed by the conventional boiling curve. The boiling curve obtained by the heat-flux-decrease technique may not exactly follow the same route as the heat-flux-increase technique (see Fig. 9). In this study, boiling hysteresis may occur under conditions of higher pool liquid temperatures such as 55°C and the foam cover thickness of 3.0 mm, which can be found in Figs. 6 and 8.

Athreya et al. [10] studied effects of heat sink orientation and metal foam geometry on the pool boiling heat transfer of FC-72 in high porosity aluminum foam heat sinks. The porosities and ppi are in the range of 90–98% and 5–40 ppi, respectively. The ppi values they used are significantly lower than those in the present paper. The foam heat sink is horizontally and vertically positioned. It is found that the inclination angles of metal foams have important influence on the pool boiling heat transfer. Hysteresis and incipience excursion are almost absent when the foam is vertically positioned. The high ppi metal foams in the high heat flux nucleate boiling regime deteriorates the heat transfer in the vertical orientation due to the significant increase of vapor flow resistance. However, the working fluid of acetone has larger latent heat of evaporation than FC-72, yielding much higher heat transfer coefficient than those reported by Athreya et al. [10] and Arbelaez et al. [16]. The deviation of the present data from Ref. [10] depends on the metal foam parameters and working fluid.

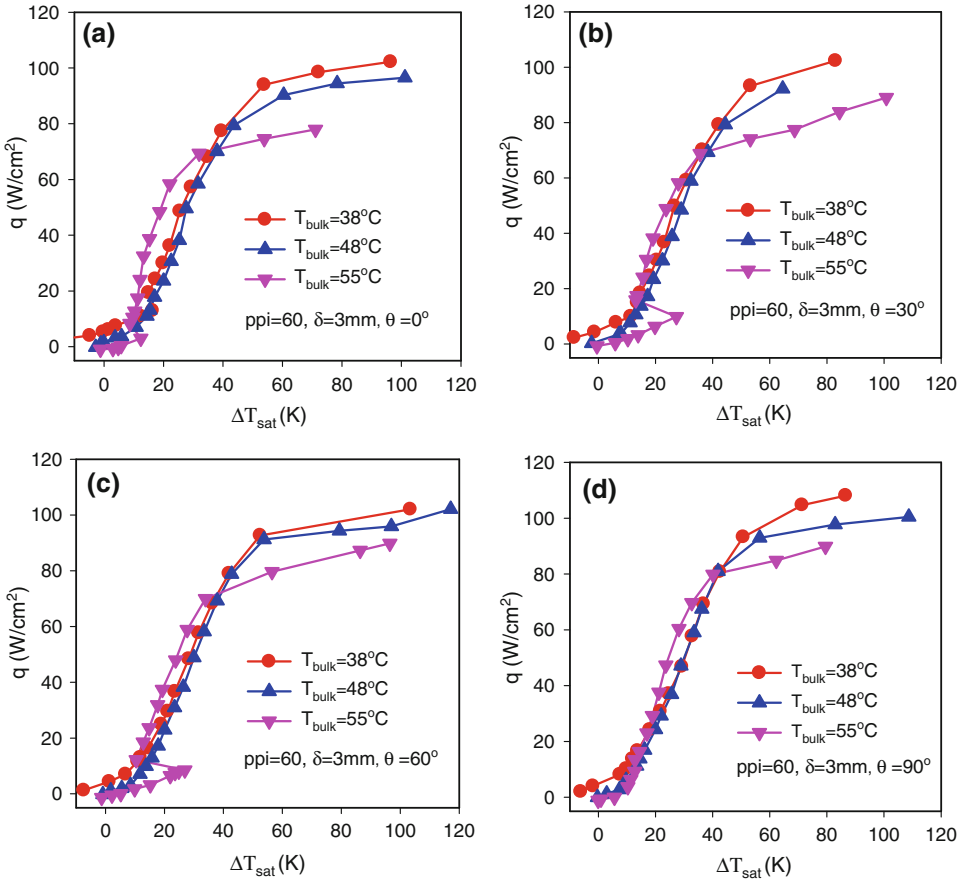

Fig. 8 Effect of pool liquid temperature on *boiling curves* at various inclination angles

3.5 Heat transfer correlation

Many studies have been carried out for the pool boiling heat transfer on porous surface. Most of them refer to the low porosity porous medium. The experimental correlation of heat transfer coefficients for the metallic foam structure is limited in the literature. There are many factors influencing the pool boiling heat transfer. These parameters will be described one by one as follow.

Inclination angle effect: Inclination angle of heating surface on the pool boiling heat transfer is represented by a parameter of ANG, which is written as

$$\mathrm{ANG} = e^{\theta/360} \tag{4}$$

where θ is the inclination angle in the range of 0–90°.

Pool liquid subcooling effect: A non-dimensional parameter describes the pool liquid subcooling effect, which is defined as

$$\Theta = \frac{T_w - T_{\mathrm{bulk}}}{T_{\mathrm{bulk}}} \tag{5}$$

where T_{w} and T_{bulk} are the wall and bulk pool liquid temperatures in the unit of K.

Vapor Reynold number effect: The generated vapor on the heating surface of foam cells causes flow disturbance in foam cells. Thus the vapor Reynolds number is defined as $Re = u_{\mathrm{v}} d_{\mathrm{p}}/v_{\mathrm{g}}$ to consider this effect on the pool boiling heat transfer, where u_{v} is the vapor velocity, d_{p} is the pore diameter, and v_{g} is the vapor kinematic viscosity. Because we have $q = m_{\mathrm{g}}/h_{\mathrm{fg}}$ and $u_{\mathrm{v}} = m_{\mathrm{g}}/(\rho_{\mathrm{g}}\varepsilon)$, the vapor Reynolds number is finally expressed as

$$Re = \frac{q d_p}{\mu_g \varepsilon h_{fg}} \tag{6}$$

where m_{g} is the vapor mass flux, h_{fg} is the latent heat of evaporation.

One may use the Grashof number to correlate the pool boiling heat transfer data. However, the Grashof number is suitable for the low heat flux condition. If the heat flux is high, such as encountered in the present paper, the boiling is violent in the porous media [9]. The flow of the vapor and liquid phases is strongly agitated, similar to a two-phase flow passing through a set of capillary tubes [25, 26]. The Reynolds number is a basic parameter describing the annular flow in capillary tube of the porous media [27]. Therefore we use the Reynolds number instead of Grashof number in this paper.

The Stefan number: The Stefan number describes the relative effect of sensible heat transfer to latent heat transfer, which is written as

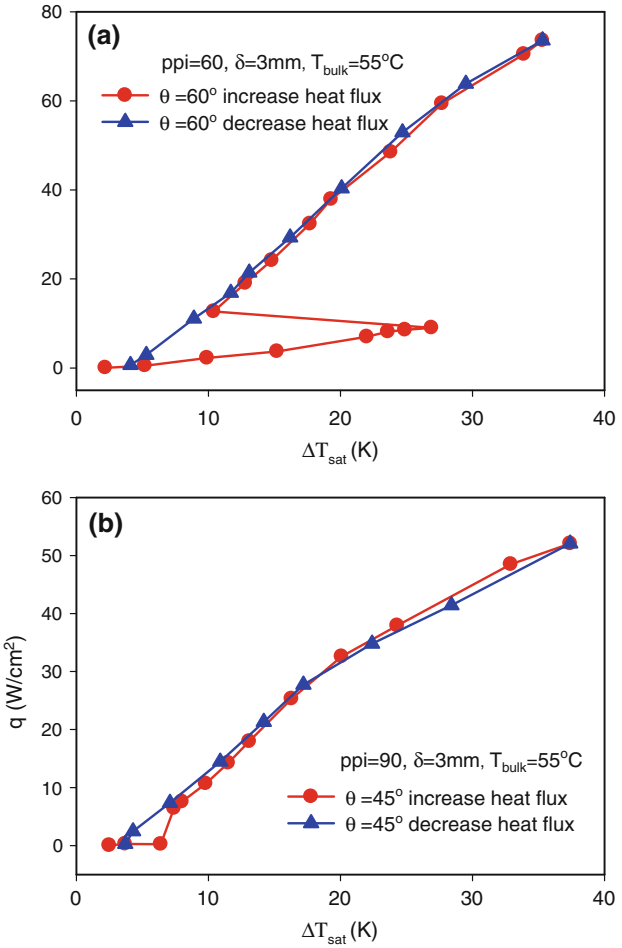

Fig. 9 Boiling hysteresis observed in the present experiment

$$Ste = \frac{C_{\mathrm{pf}}(T_w - T_{\mathrm{sat}})}{h_{fg}} \tag{7}$$

where C_{pf} is the specific heat of liquid.

The Bond number: The bond number expresses the buoyancy force effect due to the density difference between vapor and liquid phases, which is written as

$$\mathrm{Bo} = \frac{g(\rho_f - \rho_g)d_p^2}{\sigma} \tag{8}$$

Geometry size effect: It is found that foam cover thickness δ and pore diameter d_{p} have significant influence on the pool boiling heat transfer. A large foam cover thickness and/or a small pore diameter increase the bubble nucleation sites and heat transfer surface area, enhancing heat transfer. On the other hand, an increase in foam cover thickness and/or decrease in pore diameter increase the vapor release resistance, deteriorating heat transfer. Thus, a non-dimensional parameter was introduced to consider its effect on the pool boiling heat transfer as

$$F = \frac{\delta}{d_p} \tag{9}$$

Based on the above analysis, the Nusselt number is correlated as

$$Nu = CSte^{m1}Bo^{m2}Re^{m3}F^{m4}\mathrm{ANG}^{m5}\Theta^{m6} \tag{10}$$

In Eq. 10, $Nu = hd_{\mathrm{p}}/k_e$, where k_{e} is the effective thermal conductivity which is expressed as $k_e = \varepsilon k_f + A(1-\varepsilon)^n k_s$, where k_{f} and k_{s} are the liquid and solid thermal conductivities, respectively, $n = 0.763$ and $A = 0.195$, where A is cited from Ref. [16]. In Eq. 10, we neglect the effect of k_{e} and Cp_{e}, this is because only one kind of porosity (0.88) is used. Regarding the effect of d_{f}, for the same porosity of metal foam, the value of $d_{\mathrm{f}}/d_{\mathrm{p}}$ approaches a constant, thus the effect of d_{f} on the heat transfer is reflected by considering the effect of d_{p}.

Experiments in Ref. [10] had three ppi values of 5, 20 and 40 ppi and four different foam cover thicknesses. FC-72 was the working fluid with the heater surface of horizontally and vertically positioned. Incorporating the present experimental data and the data in Ref. [10], we obtain the following correlation to predict the Nusselt number:

$$Nu = 3.915 \times 10^{-3} St^{-0.214} Bo^{0.037} Re^{0.974} F^{0.038} \mathrm{ANG}^{-0.067} \Theta^{-0.715} \tag{11}$$

Figure 10 shows the comparison between the predictions by Eq. 11 and the experimental data, which comes from the present data and the data in Ref. [10]. It is seen that the

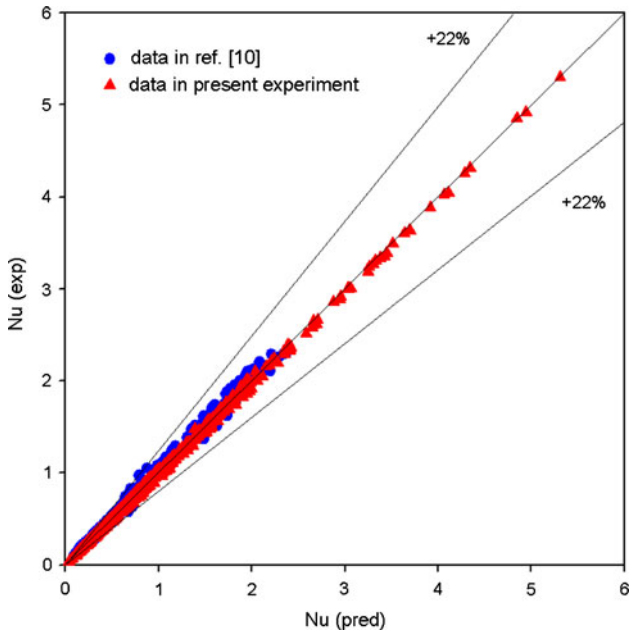

Fig. 10 Comparison between the present correlation and the experimental data

maximum error is 22%, which is acceptable for the engineering design. It is noted that the surface superheats can be up to more than 100°C in the preset study. Pool boiling heat transfer involves the nucleate boiling heat transfer mechanism and the convective heat transfer mechanism. The contribution of each heat transfer mechanism to the total heat transfer is different for different surface superheats. The wide range of surface superheats raises the difficulty to achieve high accuracy of heat transfer correlation, yielding slightly high difference between the measured Nusslet number and the predicted value, as shown in Fig. 10.

4 Conclusions

Pool boiling experiments were performed on the copper foam covers using acetone as the working fluid. The surface area is 12 mm by 12 mm. The copper foam covers have the pore densities of 30, 60, and 90 ppi, porosity of 0.88, and thicknesses of 3.0, 4.0 and 5.0 mm. The maximum heat flux that can be dissipated is up to 140 W/cm^2. The following conclusions can be drawn.

(1) Copper foam covers have low surface superheat to trigger the onset of nucleate boiling (ONB). They also have wide operation ranges of surface superheats and heat fluxes because critical heat fluxes are significantly increased, compared with smooth plain surfaces.
(2) Boiling curves are crossed between low and high inclination angles. The thermal performance becomes poorer with increases in inclination angles at small or moderate surface superheats or heat fluxes, but becomes better with increases in inclination angles at larger surface superheats or heat fluxes.
(3) Heat transfer coefficients show parabola shape, i.e., they are increased, attain maximum values, and then are decreased with continuous increases in heat fluxes.
(4) Boiling curves show small difference with the foam cover thickness in the range of 3.0, 4.0 and 5.0 mm. Generally, the thermal performance is slightly better with the foam cover thickness of 5.0 mm at small or moderate surface superheats.
(5) Influence of inclination angles on the pool boiling heat transfer is very weak at the low pool liquid temperatures.
(6) Boiling curves show small difference with the foam cover thickness from 3.0 to 5.0 mm. The thermal performance is better for the foam cover thickness of 5.0 mm if the surface superheats are smaller than 20–25 K, but it is better for the foam cover thickness of 3.0 mm if the surface superheats are larger than 20–25 K.
(7) The Nusselt number is well correlated using the 812 data points, with the maximum error of 20%.

Acknowledgments This paper is supported by the National Natural Science Foundation of China (50825603 and 50776089).

References

1. Ashby MF, Evans AG, Fleck NA, Gibson LJ, Hutchinson JW, Wadley HNG (2008) Metal foams: a design guide. Butterworth-Heinemann, Oxford
2. Degischer HP, Kriszi B (2002) Handbook of cellular metals: production, processing, applications. Wiley-VCH Verlag GmbH, Weinheim
3. Calmidi VV, Mahajan RL (1999) The effective thermal conductivity of high porosity fibrous metal foams. J Heat Transf ASME 121:466–471
4. Singh R, Kasana HS (2004) Computational aspects of effective thermal conductivity of highly porous metal foams. Appl Ther Eng 24:1841–1849
5. Zhao CY, Lu TJ, Hodson HP (2004) Thermal radiation in ultra light metal foams with open cells. Int J Heat Mass Transf 47:2939–2979
6. Boomsma K, Poulikakos D, Zwick F (2003) Metal foams as compact high performance heat exchangers. Mech Mater 35:1161–1176
7. Bhattacharya A, Mahajan RL (2006) Metal foam and finned metal foam heat sinks for electronics cooling in buoyancy-induced convection. J Electron Packag ASME 128:259–266
8. Choon NK, Chakraborty A, Aye SM, Wang XL (2006) New pool boiling data for water with copper-foam metal at sub-atmospheric pressures: experiments, and correlation. Appl Ther Eng 26: 1286–1290
9. Xu JL, Ji XB, Zhang W, Liu GH (2008) Pool boiling heat transfer of ultra-light copper foam with open cells. Int J Multiphase Flow 34:1008–1022
10. Athreya BP, Mahajan RL, Sett S, (2002) Pool boiling of FC-72 over metal foams: effect of foam orientation and geometry, 8th AIAA/ASME joint thermophysics and heat transfer conference, St. Louis, Missouri, June 24–26
11. Thome JR (1990) Enhanced boiling heat transfer, hemisphere, New York
12. Bergles AE (1997) Enhancement of pool boiling. Int J Refrig 20:545–551
13. Ingham DB, Pop I (eds) (1998) Transport phenomenon in porous media. Pergamon Press, Danvers
14. Parker JL, El-Genk MS (2005) Enhanced saturation and subcooled boiling of FC-72 dielectric liquid. Int J Heat Mass Transf 48:3736–3752
15. Arik M, Bar-Cohen A, You SM (2007) Enhancement of pool boiling critical heat flux in dielectric liquids by microporous coatings. Int J Heat Mass Transf 50:997–1009
16. Arbelaez F, Sett S, Mahajan RL (2000) An experimental study on pool boiling of saturated FC-72 in highly porous aluminum metal foams, 34th national heat transfer conference, Pittsburgh, Pennsylvania, August 20–22
17. Moghaddam S, Ohadi M (2003) Pool boiling of water and FC-72 on copper and graphite foams, proceedings of ASME InterPACK'3, international electronic packaging technical conference and exhibition, Maui, Hawaii, July 6–11

18. Nishikawa K, Fujita Y, Uchida S, Haruhiko O (1984) Effect of surface configuration on nucleate boiling heat transfer. Int J Heat Mass Transf 27:1559–1571
19. El-Genk MS, Guo S (1993) Transient boiling from inclined and downward facing surfaces in a saturated pool. Int J Refrig 16:414–422
20. El-Genk MS, Bostanci H (2003) Saturation boiling of HFE-7100 from a copper surface, simulating a microelectronic chip. Int J Heat Mass Transf 46:1841–1854
21. Chang JY, You SM (1996) Heater orientation effects on pool boiling of micro-porous-enhanced surfaces in saturated FC-72. J Heat Transf ASME 118:937–943
22. Rainey KN, You SM (2001) Effects of heater size and orientation on pool boiling heat transfer from microporous coated surfaces. Int J Heat Mass Transf 44:2589–2599
23. El-Genk MS, Parker JL (2008) Nucleate boiling of FC-72 and HFE-7100 on porous graphite at different orientations and liquid subcooling. Energy Convers Manag 49:733–750
24. Bhattacharya A, Calmidi VV, Mahajan RL (2002) Thermophysical properties of high porosity metal foam. Int J Heat Mass Transf 45:1017–1031
25. Meléndez E, Reyes R (2006) The pool boiling heat transfer enhancement from experiments with binary mixtures and porous heating covers. Exp Therm Fluid Sci 30:185–192
26. Shi MH, Zhao YB, Liu ZL (2003) Study on boiling heat transfer in liquid saturated particle bed and fluidized bed. Int J Heat Mass Transf 46:4695–4702
27. Suo M, Griffith P (1964) Two-phase flow in capillary tubes. J Basic Eng 86:576–582